Effect of $In_xGa_{1-x}N$ "continuously graded" buffer layer on InGaN epilayer grown by metalorganic chemical vapor deposition*

Qian Wei-Ning(钱卫宁)[a)b)], Su Shi-Chen(宿世臣)[a)], Chen Hong(陈 弘)[b)†], Ma Zi-Guang(马紫光)[b)], Zhu Ke-Bao(朱克宝)[a)], He Miao(何 苗)[a)‡], Lu Ping-Yuan(卢平元)[a)], Wang Geng(王 耿)[a)], Lu Tai-Ping(卢太平)[b)], Du Chun-Hua(杜春花)[b)], Wang Qiao(王 巧)[a)], Wu Wen-Bo(吴汶波)[a)], and Zhang Wei-Wei(张伟伟)[a)]

[a)] *Laboratory of Nanophotonic Functional Materials and Devices, Institute of Opto-electronic Materials & Technology, South China Normal University, Guangzhou* 510631, *China*

[b)] *Key Laboratory for Renewable Energy, Chinese Academy of Sciences, Beijing Key Laboratory for New Energy Materials and Devices, Beijing National Laboratory for Condense Matter Physics, Institute of Physics, Chinese Academy of Sciences, Beijing* 100190, *China*

(Received 4 January 2013; revised manuscript received 20 March 2013)

In this paper we report on the effect of an $In_xGa_{1-x}N$ continuously graded buffer layer on an InGaN epilayer grown on a GaN template. In our experiment, three types of buffer layers including constant composition, continuously graded composition, and the combination of constant and continuously graded composition are used. Surface morphologies, crystalline quality, indium incorporations, and relaxation degrees of InGaN epilayers with different buffer layers are investigated. It is found that the $In_xGa_{1-x}N$ continuously graded buffer layer is effective to improve the surface morphology, crystalline quality, and the indium incorporation of the InGaN epilayer. These superior characteristics of the continuously graded buffer layer can be attributed to the sufficient strain release and the reduction of dislocations.

Keywords: InGaN, reciprocal space map, indium incorporation, surface morphology

PACS: 61.72.uj, 68.35.Dv, 68.37.Ps, 78.60.Lc **DOI:** 10.1088/1674-1056/22/10/106106

1. Introduction

Hetero-epitaxial growth has been an important subject for III/V compound semiconductors. Researchers can obtain an optoelectronic device with good performance by integrating dissimilar material for bandgap engineering. However, hetero-epitaxial growth usually brings a lot of problems including defect, phase separation, deteriorated surface, and crystalline quality,[1,2] owing to different material properties such as thermal expansion coefficient and lattice constant.[3] These problems are serious especially for InGaN grown on GaN template. Therefore, it is an important issue for fabricating high performance devices to reduce the dislocation density and improve the film quality of InGaN.

The buffer layer technology[4] is a suitable technique to minimize the effect of lattice mismatch in a hetero-epitaxial system for improving the epilayer quality. This technology has been a standard route to improving material quality in a range of material systems like SiGe,[5] InGaAs/GaAs,[5,6] and GaAs/Si.[7] For the group III-nitrides, especially InGaN grown on GaN template, a step-graded buffer layer is used to improve the quality of the epilayer, however there are few reports dealing with the continuously graded buffer layer and no detailed understanding of this buffer layer technique is available.

In this study, the $In_xGa_{1-x}N$ continuously graded buffer layer is employed to improve the indium incorporation efficiency and InGaN epilayer quality by sufficient strain release and the dislocation reduction. The atomic force microscope (AFM) and low temperature photoluminescence (PL) spectra are used for measuring the surface morphologies and the crystalline quality. The reciprocal space maps (RSM) of the InGaN epilayers with different buffer layers are measured to investigate the indium composition and relaxation degree.

2. Experiment

A 300-nm InGaN epilayer combined with 2-μm GaN was grown on sapphire by metalorganic vapor phase epitaxy (MOVPE). Trimethygallium (TMGa), trimethlindium (TMIn), and ammonia (NH_3) were used as the Ga, In, and N sources, respectively. Nitrogen was used as the carrier gas to achieve high quality InGaN. Prior to the growth, the sapphire substrate was annealed to remove residual impurities on the surface in an H_2 ambient environment at 1030 °C. A 25-nm-thick GaN nucleation layer was first deposited on the sapphire substrate at 540 °C with subsequent growth of high temperature 2-μm GaN template at 1020 °C. Following the GaN template, a 200-nm InGaN buffer layer with different styles was deposited us-

*Project supported by the National High Technology Research and Development Program of China (Grant Nos. 2011AA03A112, 2011AA03A106, and 2013AA03A101), the National Natural Science Foundation of China (Grant Nos. 11204360, 61210014, and 61078046), the Science & Technology Innovation Program of the Department of Education of Guangdong Province, China (Grant No. 2012CXZD0017), the Industry–Academia-Research Union Special Fund of Guangdong Province, China (Grant No. 2012B091000169), and the Science & Technology Innovation Platform of Industry–Academia-Research Union of Guangdong Province–Ministry Cooperation Special Fund, China (Grant No. 2012B090600038).

†Corresponding author. E-mail: hchen@aphy.iphy.ac.cn

‡Corresponding author. E-mail: herofate@126.com

© 2013 Chinese Physical Society and IOP Publishing Ltd

ing optimized deposition parameters. Finally, the 300-nm InGaN epilayer was deposited. The composition of 300-nm InGaN epilayer grown directly on GaN template was about 7%.

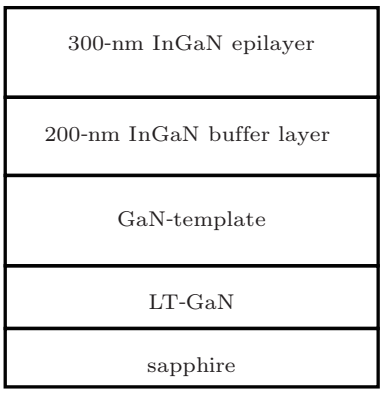


Fig. 1. Schematic plot of InGaN sample with different buffer layers.

The schematic diagram of InGaN epilayer with buffer layer is shown in Fig. 1. Three samples have the same structure except the 200-nm buffer layer, which are labeled as samples A, B, and C, respectively. For sample A, the buffer layer is a 200-nm 7% constant composition InGaN layer. For sample B, the buffer layer consists of 100 nm compositionally graded from 0% to 7% $In_xGa_{1-x}N$ layer and 100-nm 7% constant composition InGaN layer. For sample C, the buffer layer is only 200-nm $In_xGa_{1-x}N$ entirely continuously graded layer, where x varies between 0% and 7%.

3. Results and discussion

The surface morphologies of InGaN epilayers are investigated by AFM as shown in Fig. 2. The island-like surfaces are clearly visible in samples A and B, indicating the three-dimensional (3D) growth mode of the two samples. The

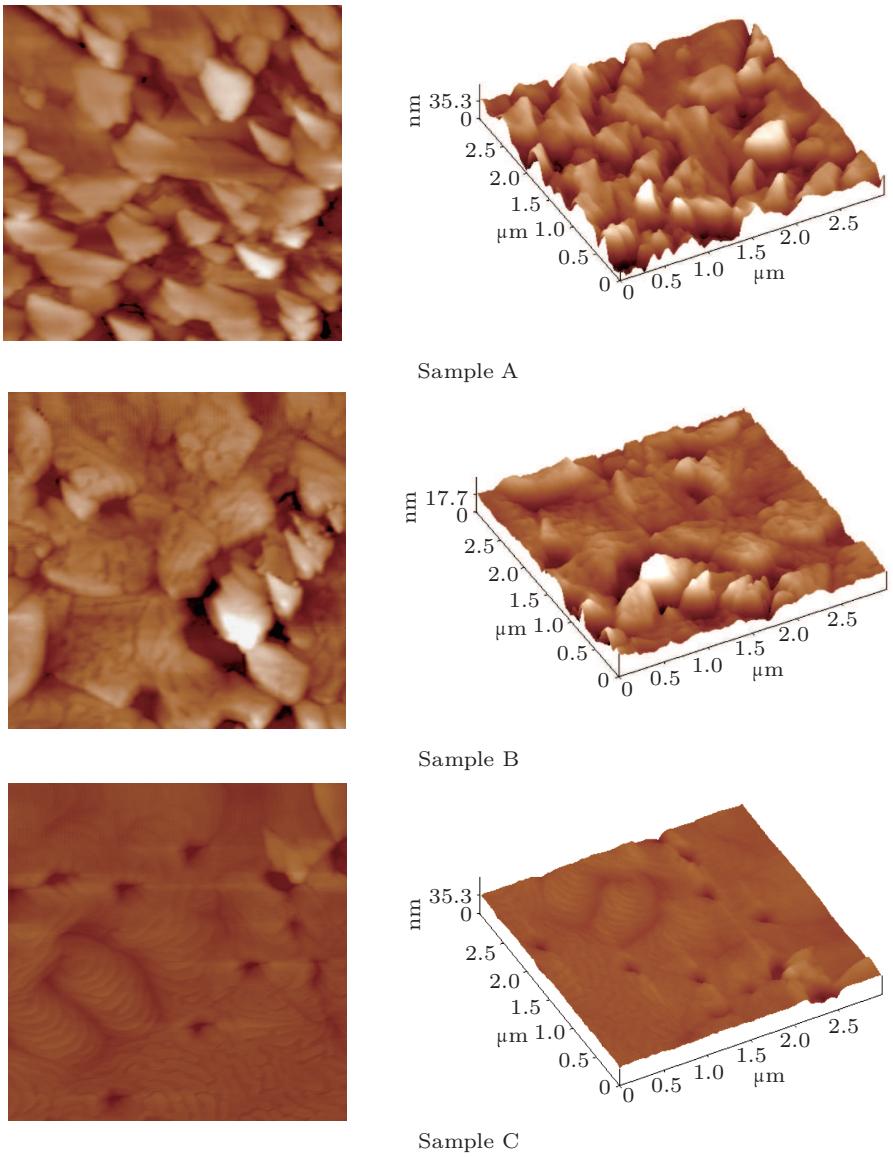


Fig. 2. (color online) 2D and 3D AFM images of three samples.

estimated root-mean-square (RMS) surface roughness of the two samples are 11.3 nm and 5.2 nm, respectively. The RMS surface roughness of sample C is 2.6 nm, showing much smoother surface morphology with two-dimensional (2D) growth mode. Generally, strain-induced surface roughening is the dominant mechanism for strain energy release. Combined with surface roughness of the samples, the strain energy in sample C is smaller than those in samples A and B. This effect may be caused by two reasons. The first one is that the average indium composition of the $In_xGa_{1-x}N$ continuously graded $In_xGa_{1-x}N$ buffer layer is lower than that of the constant composition buffer layer; the second one is that the continuously graded buffer layer can release the strain more sufficiently than the constant composition buffer layer.

The (002) ω-scan of high resolution X-ray diffraction (XRD) and low temperature PL are measured to characterize the crystalline quality of the InGaN epilayer.[8] The indium content values in these samples are evaluated by the separation between GaN and InGaN peaks in the XRD spectra as shown in Fig. 3. Sample C has the highest average indium composition in the three samples. Figure 4 shows the comparison of low temperature PL spectrum among the three samples. The PL spectra are measured using the same optical path for each sample. It is obvious that the PL intensity of sample C is superior to those of the other two samples. The corresponding low temperature PL full width at half maximum (FWHM) values and (002) XRD FWHM values of the InGaN epilayers for the three samples are shown in Table 1. Sample C has the best crystalline quality of the three samples. It is clear from the above results that the reduction of dislocation density in the continuously graded buffer layer sample is responsible for the improvement of the crystalline quality. Our results are in good agreement with the reported results of Niu *et al.*[9] They observed the shift of PL peak towards shorter wavelength due to the insertion of the graded layer.

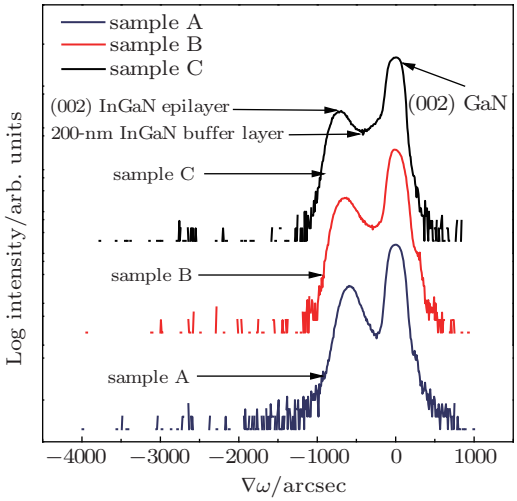


Fig. 3. (color online) XRD spectra of three samples.

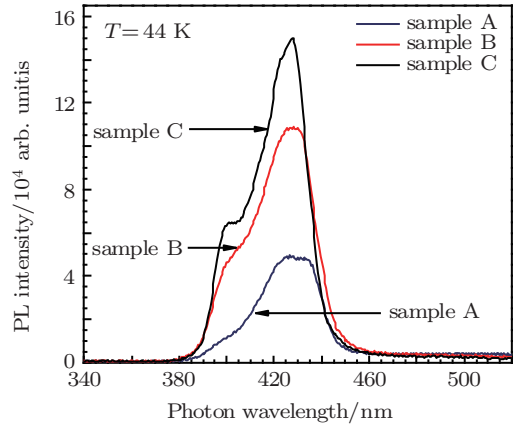


Fig. 4. (color online) PL spectra of three samples.

Table 1. Corresponding low temperature PL full width at half maximum (FWHM) values and (002) XRD FWHM values of the InGaN epilayers for the three samples.

Materials	Buffer layer structure	Ra/nm	RMS/nm	InGaN(002) FWHM/arcsec	PL FWHM/nm
Sample A	200 nm (constant composition)	8.9	11.3	754	24.7
Sample B	100 nm (graded)+100 nm (constant)	3.74	5.2	644	19.6
Sample C	200 nm (graded composition)	1.66	2.6	550	16.6

The information about indium component and the strain of an epitaxial film can be obtained by performing an RSM on an asymmetric reflection using a double-crystal XRD system.[10] Reciprocal space coordinate Q_x and Q_y of the InGaN reciprocal lattice point (RLP) are directly related to the lattice constants a and c. Knowing the lattice parameters, it is possible to estimate the InN content x and strain statues by finding physically acceptable solutions of the 2D Poisson ratio equation.[11] The following input parameters required for the solution of the Poisson equation are used: the lattice parameters are a_0(GaN) = 3.1892 Å and c_0(GaN) = 5.1850 Å for GaN,[12] and a_0(InN) = 3.5378 Å and c_0(InN) = 5.7033 Å for InN,[13] and elasticity coefficients are $c_{13} = 103$ GPa and $c_{33} = 405$ GPa for GaN,[13] and $c_{13} = 92$ GPa, $c_{33} = 224$ GPa for InN.[13]

Asymmetrical RSMs of the three samples measured around the (105) reflection are shown in Fig. 5. The relative positions ∇Q_x and ∇Q_y to GaN RLP corresponding to samples A, B, and C are $(-2.5 \times 10^{-3}, -6.5 \times 10^{-2})$, $(-2.5 \times 10^{-3}, -6.7 \times 10^{-2})$, and $(-4 \times 10^{-3}, -7 \times 10^{-2})$, respectively. By

solving the 2D Poisson ratio equation,[11] indium components and relaxation degrees of the InGaN epilayers for samples A, B, and C are 7.28%, 7.49%, 8.03%, and 13.69%, 14.12%, 19.94%, respectively.

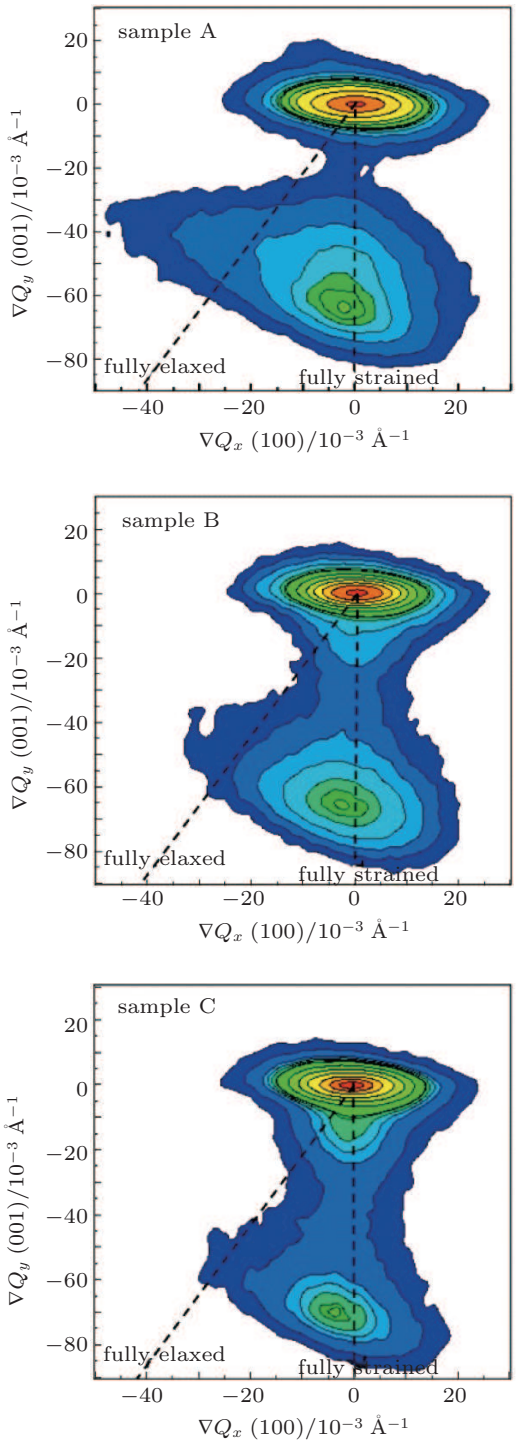


Fig. 5. (color online) Asymmetrical RSMs measured around the (105) reflection of three samples.

Due to the lattice mismatch (10.6% between GaN and InN) and thermal expansion coefficients mismatch (28% between GaN and InN), a large compressive strain exists in the InGaN epilayer grown on GaN template, which suppresses the incorporation of indium. Due to composition pulling effect, enhanced strain leads to lower indium incorporation.[14] A similar effect has been reported in liquid phase epitaxy (LPE) growth of InGaP/GaAs and InGaP/GaAsP systems[15] and molecular beam epitaxy (MBE) growth of an AlInAs/InP system.[16] Based on the above asymmetrical RSM results, indium incorporation of InGaN epilayer in sample C is higher than in samples A and B. The epilayer of sample C shows more relaxed structure than those of the other samples. The results about indium composition and the strain state are in coincidence with the results of XRD and surface morphologies. In view of the above discussion, we may conclude that the continuously graded buffer layer can release the strain effectively compared with the constant composition buffer layer.

Based on the Matthews–Blakeslee balance force model,[17] the critical layer thickness is inversely dependent on indium composition and the misfit strain. Hence, a continuous increase in indium composition leads to a larger critical thickness in the upper layer, which ceases the rapid increase in mismatch dislocation, and much fewer dislocations are transported into the InGaN epilayer. Meanwhile, an accommodation of strain is existent in the compositional gradation process. In the growth process of the continuously graded buffer layer, the strain can be gradually released by the atomic migration and dislocation glide instead of being accumulated in the buffer layer. Finally, the strain is reduced and indium incorporation is increased in the InGaN epilayer. However, for the constant composition buffer layer, there is neither accommodation of the strain nor the reduction of threading dislocation. The surface and crystalline quality of the InGaN epilayer are inferior to those of the sample with the continuously graded buffer layer, and the indium incorporation is lower than that of the sample with the continuously graded buffer layer. Therefore, we can achieve a smooth surface, good crystalline quality, and high indium composition InGaN epilayer by using the continuously graded InGaN buffer layer.

4. Conclusions

The effects of continuous buffer layer on the InGaN epilayer are studied. By comparing with constant composition buffer layer, we find that the continuously graded buffer layer can improve the surface morphology and crystalline quality and can increase indium incorporation. The continuously graded InGaN buffer layer acts as a “transition layer” between InGaN epilayer and GaN template. This layer can release the strain and reduce the dislocations in the InGaN epilayer. The lower dislocation density, lower residual strain, and higher indium incorporation in the InGaN epilayer than in the constant composition layer, make the continuously graded layer a superior technique for fabricating the high performance semiconductor devices.

References

[1] Yang P F, Jian S R, Lai Y S, Yang C S and Chen R S 2008 *J. Alloys Compd.* **463** 533

[2] Zhang D Y, Zheng X H, Li X F, Wu Y Y, Wang H, Wang J F and Yang H 2012 *Chin. Phys. B* **21** 087802

[3] Kawaguchi Y, Shimizu M, Yamaguchi M, Hiramatsu K, Sawaki N, Taki W, Tsuda H, Kuwano N, Oki K, Zheleva T and Davis R F 1998 *J. Crystal Growth* **189** 24

[4] Jiang Y, Luo Y, Xi G Y, Wang L, Li H T, Zhao W and Han Y J 2009 *Acta Phys. Sin.* **58** 7282 (in Chinese)

[5] Legoues F K, Meyerson B S, Morar J F and Kirchner P D 1992 *J. Appl. Phys.* **71** 4230

[6] Schlenker D, Miyamoto T, Chen Z, Koyama F and Iga K 1999 *IEEE Photon. Technol. Lett.* **11** 946

[7] Takano Y, Hisaka M, Fujii N, Suzuki K, Kuwahara K and Fuke S 1998 *Appl. Phys. Lett.* **73** 2917

[8] Zhao W, Wang L, Wang J X and Luo Y 2011 *Chin. Phys. B* **20** 076101

[9] Niu N H, Wang H B, Liu J P, Liu N X, Xing Y H and Han J 2006 *J. Crystal Growth* **286** 209

[10] Guo X, Wang H, Jiang D S, Wang Y T, Zhao D G, Zhu J J, Liu Z S, Zhang S M and Yang H 2012 *Chin. Phys. B* **21** 068102

[11] Pereira S, Correia M R, Pereira E, O'Donnell K P, Alves E, Sequeira A D and Franco N 2001 *Appl. Phys. Lett.* **79** 1432

[12] Detchprohm T, Hiramatsu K, Itoh K and Akasakic I 1992 *Jpn. J. Appl. Phys.* **2** 31

[13] Kachkanov V, Dolbnya I P, O'Donnell K P, Martin R W, Edwards P R and Pereira S 2011 *Appl. Phys. Lett.* **99** 1909

[14] Stringfellow G B 1972 *J. Appl. Phys.* **43** 3455

[15] Ohta J, Ishikawa M, Ito R and Ogasawara N 1983 *Jpn. J. Appl. Phys.* **22** L136

[16] Allovon M, Primot J, Gao Y and Quillec M 1989 *Electron J. Mater.* **18** 505

[17] Srinivasan S, Geng L, Liu R, Ponce F A, Narukawa Y and Tanaka S 2003 *Appl. Phys. Lett.* **83** 5187